Condensed Matter Physics, 2011, Vol. 14, No 2, 23701: 1–13
DOI: 10.5488/CMP.14.23701
http://www.icmp.lviv.ua/journal

CONDENSED MATTER PHYSICS

A comparative study for structural and electronic properties of single-crystal ScN

R. Mohammad[1,2], Ş. Katırcıoğlu[2]

[1] Palestine Technical University, Applied Science College, WestBank, Palestine

[2] Middle East Technical University, Physics Department, 06530 Ankara, Turkey

Received November 4, 2010, in final form February 3, 2011

A comparative study by FP-LAPW calculations based on DFT within LDA, PBE-GGA, EV_{ex}-PW_{co}-GGA, and EV_{ex}-GGA-LDA_{co} schemes is introduced for the structural and electronic properties of ScN in RS, ZB, WZ, and CsCl phases. According to all approximations used in this work, the RS phase is the stable ground state structure and makes a transition to CsCl phase at high transition pressure. While PBE-GGA and EV_{ex}-PW_{co}-GGA's have provided better structural features such as equilibrium lattice constant and bulk modulus, only EV_{ex}-PW_{co}-GGA and EV_{ex}-GGA-LDA_{co}'s have given the non zero, positive indirect energy gap for RS-ScN, comparable with the experimental ones. The indirect band gap of ScN in RS phase is enlarged to the corresponding measured value by EV_{ex}-PW_{co}-GGA+U^{SIC} calculations in which the Coulomb self and exchange-correlation interactions of the localized d-orbitals of Sc have been corrected by the potential parameter of U. The EV_{ex}-PW_{co}-GGA calculations have also provided good results for the structural and electronic features of ScN in ZB, WZ, and CsCl phases comparable with the theoretical data available in the literature. EV_{ex}-PW_{co}-GGA and EV_{ex}-PW_{co}-GGA+U^{SIC} schemes are considered to be the best ones among the others when the structural and electronic features of ScN are aimed to be calculated by the same exchange-correlation energy approximations.

Key words: *ScN, FP-LAPW, DFT, structural properties, electronic properties*

PACS: *71.15.Mb, 71.15.Nc, 71.20.Nr, 71.18.+y*

1. Introduction

ScN (Scandium nitride) has many potential applications due to its high mechanical strength [1], good thermal stability with a melting temperature above 2000° C [2] and high hardness of 21 GPa with respect to load deformation [1]. After the epitaxial growth of smooth and singly oriented ScN films [1–8], ScN was also considered to be a potential semiconductor in electronic device applications. X-Ray diffraction analysis indicated that, unlike the other nitride semiconductors, all ScN films crystallize into a single rock-salt (RS) phase (B1) with a lattice constant of ∼4.5 Å [1, 3–8]. The RS structure was also determined to be the most stable structure for ScN by the comparative theoretical works [9–11]. The lattice constant of ScN in RS phase has been calculated to be in the range of 4.42–4.651 Å [9, 11–15] by the first principles calculations within local density approximation (LDA) [16, 17] and generalized gradient approximation (GGA) [18, 19] of exchange and correlation energies. In these works [9–14], the bulk modulus of ScN has been reported in the range of 196–235 GPa with respect to the experimental value of 182∓40 [1]. In the literature the most stable RS phase with the cohesive energy of –13.69 [9] and –13.428 eV [10] was found to be followed by the wurtzite (WZ or B4), zinc-blende (ZB or B3), and CsCl (B2) type meta-stable structures of ScN with the ordered cohesive energies of –13.35 [9], –13.03 [9], and –11.58 eV [9] (–11.34 eV [10]), respectively. These cohesive energies correspond to the lattice constants of 3.49 ($c/a = 1.6$, $u = 0.38$) [9], 4.88 [9] and 2.81 Å [9] (2.79 Å [10]) for WZ, ZB, and CsCl phases of ScN, respectively. In a recent work [11], the lattice constants have been calculated to be 3.45, 4.939, and 2.926 Å for ScN in WZ, ZB and CsCl phases. The bulk modulus of WZ phase of ScN has been reported to be 156 [9] and 132.91 GPa [11] by GGA and LDA of exchange and correlation energies, respectively. In the same works, the bulk modulus of CsCl phase was calculated to be 170 [9] and

159.759 GPa [11]. In another work [10], the CsCl meta-stable phase of ScN has the bulk modulus of 178.60 GPa by GGA calculations.

The first principles electronic band structure calculations within LDA [9, 11, 12, 14] and GGA [9, 10, 13] schemes indicated that RS-ScN was a semi-metal with an almost zero indirect band gap. However, ScN in RS phase was a semiconductor with the indirect gap of 2.4 [8], 1.3∓0.3 [20], and 0.9∓0.1 eV [7] measured by optical transmission, reflection and absorption experiments, respectively. The recent ab-initio calculations [12, 14, 15, 20, 21] using pseudopotential (PP) method within Hedin's [22] Green's functions quasiparticle corrections on LDA (LDA-G_oW_o), exact exchange of LDA [23] [OEPx(cLDA)], and Hedin's Green's functions quasiparticle corrections on exact exchange of LDA [OEPx(cLDA)-G_oW_o], Linear Muffin Tin Orbital (LMTO) method within Bechstedt's [24] Green's functions quasiparticle corrections on LDA (LDA-GW) and full-potential-linearized augmented plane waves (FP-LAPW) method within GGA [19] and screened exchange of LDA (sx-LDA) [25] have all supported the semiconductor nature of the stable ScN by giving the indirect gap in the range of 0.54–1.70 eV at X symmetry point ($E_g^{\Gamma-X}$). In [12, 14, 20, 21], the optical direct gap of RS structure at X point (E_g^{X-X}) was calculated in the range of 1.98–2.90 eV with respect to the experimental direct absorptions in the range of 1.8–2.4 eV [3, 4, 7, 8, 20].

The recent DFT calculations within GGA scheme [9] have indicated that the WZ and ZB meta-stable structures of ScN were non-metallic with large indirect gaps of ∼3 eV along M-Γ symmetry line ($E_g^{M-\Sigma}$) and 2.3 eV at W symmetry point (E_g^{X-W}), respectively. The nonmetallic nature of ScN in ZB phase was also obtained by an indirect gap of 2.36 eV at W point (E_g^{X-W}) by LDA scheme [11]. These GGA and LDA calculations of ScN in ZB phase [9, 11], have given the direct gap of 2.4 and 2.42 eV at X symmetry point, respectively. In the literature, ScN in B2 phase was reported to be metallic by DFT calculations within GGA [9, 10] and LDA [11] schemes.

In the literature, although ScN has not been worked so far, hybrid FP-LAPW calculations within the framework of DFT and different exchange-correlation functionals have given accurate electronic features for nitride compounds and alloys [26, 27] comparable with the corresponding measured ones due to the possible strong hybridization between the $2p$ orbitals of N and the corresponding cationic states. In addition, the orthogonalized norm-conserving pseudopotential (NCPP) method in which the plane wave basis functions are orthogonalized to core-like orbitals has been reported to be a very promising method in electronic band structure calculations of nitride alloys [28] for describing the experimental optical data, together with the FP-LAPW method within virtual crystal approximation [28].

In the present work, we have examined the structural and electronic properties of ScN in stable (RS) and meta-stable phases (CsCl, ZB, WZ) by DFT calculations mainly within two GGA schemes which have not been used before for ScN. We have aimed to introduce a comparative study for the structural and electronic features of ScN such as the lattice constant, bulk modulus, cohesive energy, energy gaps and the effective masses of electrons and holes. The present work has also comprised the electronic band structure of stable ScN corrected by an on-site Coulomb self- and exchange-correlation potential approximation (U^{SIC}) [29].

2. Method of calculations

The present DFT calculations on the structural and electronic properties of ScN compound have been performed using FP-LAPW method implemented in WIEN2k code [30]. In the literature, the exchange-correlation energy of DFT has been defined by local density approximation (LDA) [16] for the systems having uniform electron charge density. But for the systems of non-uniform charge density, the exchange-correlation energy of LDA has been corrected by gradient of the charge density within different generalized gradient approximations (GGA). In the present total energy and electronic band structure calculations of ScN in B1-B4 phases, four different approximations of exchange-correlation energies have been considered. In one of the approximations, exchange and correlation energies have been defined simply by LDA [16], without regarding the homogeneity of the real charge density. In the second approximation, exchange and correlation energies of LDA have been corrected by GGA of Perdew-Burke-Ernzerhof (PBE) [19]. The generalized gradient functional

of Perdew-Burke-Ernzerhof [19] has retained correct features of LDA [16] and satisfied only those which are energetically significant. In the third approximation, GGA of Engel-Vosko (EV) [31] and GGA of Perdew and Wang (PW) [32] have been used to correct the exchange and correlation energies, respectively. Since the generalized gradient functional of Engel-Vosko [31] was designed to give a better exchange potential (V_{x}) only, the standard correlation potential of LDA [16] in the third approximation has been corrected by another functional, namely, GGA of Perdew and Wang [32]. The functional of Perdew and Wang [32] has incorporated some inhomogeneity effects while retaining many of the best features of the local density approximation. In the last approximation, the exchange energy of LDA [16] was corrected by GGA of Engel-Vosko [31], but the correlation energy was defined directly by LDA [16]. The exchange-correlation energy approaches considered in this work have been labeled as LDA, PBE-GGA, $\mathrm{EV_{ex}}$-$\mathrm{PW_{co}}$-GGA and $\mathrm{EV_{ex}}$-GGA-$\mathrm{LDA_{co}}$. The acronyms have been produced either based on the key word of the approach (LDA) or on the name of the authors (PBE-GGA, $\mathrm{EV_{ex}}$-$\mathrm{PW_{co}}$-GGA, $\mathrm{EV_{ex}}$-GGA-$\mathrm{LDA_{co}}$) who developed the corresponding exchange and correlation functionals. Here, the subscripts of exchange (ex) and correlation (co) functionals are exclusively used for the cases where the exchange and correlation functionals are different. It has been considered that $\mathrm{EV_{ex}}$-$\mathrm{PW_{co}}$-GGA and $\mathrm{EV_{ex}}$-GGA-$\mathrm{LDA_{co}}$ schemes can provide significant improvement for the structural and electronic properties of ScN, respectively. In the literature, it was reported that LDA+U and GGA+U schemes can also improve the band gap energies of transition metal compounds and alloys by reproducing quite well the localized nature of the d-electrons (or f-electrons) [33–35]. Since the ab-initio calculations are difficult to perform, the strong correlations like in transition metal compounds and alloys are often based on a model Hamiltonian approach in which the important parameter of U improves the effective Coulomb interactions between the localized d-electrons. In the present work, the electronic band structure of RS-ScN calculated by $\mathrm{EV_{ex}}$-$\mathrm{PW_{co}}$-GGA has been improved by $\mathrm{U^{SIC}}$ method [29, 36] introduced in WIEN2k code [30]. The present $\mathrm{EV_{ex}}$-$\mathrm{PW_{co}}$-GGA+$\mathrm{U^{SIC}}$ scheme has rectified on-site Coulomb self- and exchange-correlation interactions of the localized d-orbitals of Sc by the potential parameter of U [29, 36]. In Anisimov et al's paper [29], the meaning of the U parameter were defined as the cost Coulomb energy for the placement of two d-electrons on the same site. The Coulomb interaction was defined to be $(1/2)\mathrm{U}\sum_{i\neq j}\mathrm{n}_i\mathrm{n}_j$ [37] for d-orbitals. Here, n_i are d-orbital occupancies. The Coulomb interaction term included into the total energy functional of $\mathrm{EV_{ex}}$-$\mathrm{PW_{co}}$-GGA has given the orbital energies of ScN as $\xi_i{=}\xi_{(\mathrm{EV_{ex}}-\mathrm{PW_{co}}-\mathrm{GGA})}{+}\mathrm{U}(1/2-n_i)$ [37]. The shifting of the corresponding orbital energies in $\mathrm{EV_{ex}}$-$\mathrm{PW_{co}}$-GGA+$\mathrm{U^{SIC}}$ calculations gives a qualitative improvement for the energy gap of RS-ScN. The present Coulomb interaction parameter of U is calculated to be 4.08 eV in WIEN2k [30] to have the maximum approach to the measured indirect band gap of RS-ScN.

In the present work, ScN has been studied in RS, CsCl, ZB, and WZ structures. The unit cells of RS, CsCl, and ZB consist of two basis atoms; Sc at (0, 0, 0) and N at ($0.5a$, $0.5a$, $0.5a$) in fcc structure, Sc at (0, 0, 0) and N at ($0.5a$, $0.5a$, $0.5a$) in bcc structure, and Sc at (0, 0, 0) and N at ($0.25a$, $0.25a$, $0.25a$) in fcc structure, respectively, where a is the lattice constant parameter. The WZ structure with space group of $F6_3mc$ has four atoms in the unit cell; Sc atoms at ($a/3$, $2a/3$, 0) and ($2a/3$, $a/3$, $0.5c$), N atoms at ($a/3$, $2a/3$, $u*c$) and ($2a/3$, $a/3$, $(0.5+u)*c$), where a and c are the periods in x-y plane and along z direction, respectively. The z directional distance, u, is defined between the layers of Sc and N atoms. In FP-LAPW calculations, each unit cell is partitioned into non-overlapping muffin-tin spheres around the atomic sites. Basis functions are expanded in combinations of spherical harmonic functions inside the non-overlapping spheres. In the interstitial region, a plane wave basis is used and expansion is limited with a cutoff parameter, $R_{\mathrm{MT}}K_{\mathrm{MAX}}{=}7$. Here, R_{MT} is the smallest radius of the sphere in the unit cell, K_{MAX} is the magnitude of the largest K vector used in the plane wave expansion. The muffin-tin radius is adopted to be 1.8 and 1.67 a.u. for Sc and N atoms, respectively. In the calculations, the electrons of Sc and N atoms in $3s^2 3p^6 4s^2 3d^1$ and $2s^2 2p^5$ shells respectively, are treated as valence electrons by choosing a cutoff energy of –6.0 Ry. The core states are treated within the spherical part of the potential only and are assumed to have a spherically symmetric charge density totally confined inside the muffin-tin spheres. The expansion of spherical harmonic functions inside the muffin-tin spheres is truncated

at l=10. The cutoff for Fourier expansion of the charge density and potential in the interstitial region is fixed to be $G_{\mathrm{MAX}} = 16\sqrt{\mathrm{Ry}}$. The FP-LAPW parameters presented in this work have been obtained after a few trials around their fixed values.

The ScN in RS, CsCl and ZB structures have been optimized with respect to the volume of the unit cells by minimizing the total energy. The equilibrium lattice constants of ScN in RS, CsCl, and ZB phases are determined by fitting the total energies to the Murnaghan's equation of state [38]. The equilibrium structure of ScN in WZ phase that corresponds to the minimum total energy has been obtained by the application of both volume and geometry optimizations. The volume optimization used for all structures is provided with the energy criterion of 0.01 mRy. The optimum volume for WZ phase corresponds to the optimum c/a ratio and a value has been found by fitting the total energies to a quadratic function in a least square fitting method. The z directional distance u between the Sc and N layers in WZ phase has been obtained by geometry optimization at the optimum volume of the unit cell. The geometry optimization forces the atoms in the unit cell to move towards their equilibrium positions. In the geometry optimization, all forces on the atoms are converged to less than 1 mRy/a.u. The variation of total energy with respect to the volume and c/a ratio of WZ structure is plotted in figure 1. The present structural and electronic band calculations have been performed using 21x21x21 grids and correspond to 1000 k points sufficiently defined in the irreducible wedge of the Brillouin zone for ScN in B1-B4 phases.

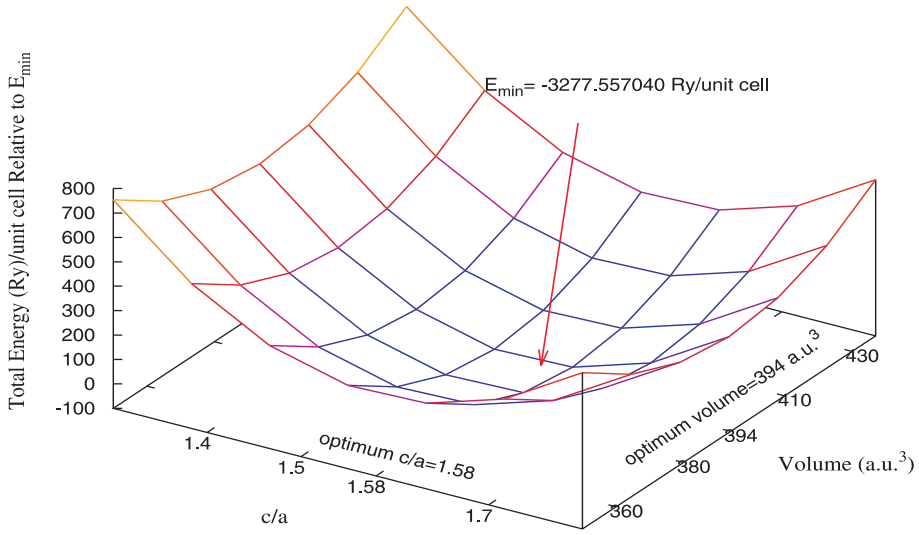

Figure 1. (Color on-line) The relative total energy (per unit cell) versus volume and c/a within $\mathrm{EV_{ex}}$-$\mathrm{PW_{co}}$-GGA for WZ-ScN.

In the present work, the cohesive energies (energy/atom-pair) of ScN structures (B1-B4) have been calculated by

$$E_{\mathrm{coh.}} = E_{\mathrm{ScN}} - ME_{\mathrm{N}} - ME_{\mathrm{Sc}}\,. \tag{2.1}$$

Where, $\mathrm{E_N}$ and $\mathrm{E_{Sc}}$ are the values of the self-atomic energies of N and Sc atoms. $\mathrm{E_{ScN}}$ is the minimum of the total energy per unit cell that corresponds to the equilibrium structures of the ScN phases. Here, M defines the number of N and Sc atoms in the unit cell of the phases. The self-atomic energies of either atoms are calculated accurately in a fcc super cell with a lattice constant of 25 a.u.

3. Results and discussion

3.1. Structural properties

The total energies (per unit cell) of RS, CsCl, WZ and ZB structures of ScN calculated within EV_{ex}-PW_{co}-GGA scheme are plotted as a function of the volume of the structures in figure 2. The curvature of variations is made clear by plotting the total energies (per unit cell) of the structures relative to the minimum total energy of the RS-ScN. The minimum of the total energies of the phases with E(RS-ScN)<E(WZ-ScN)<E(ZB-ScN)<E(CsCl-ScN) rank indicates that the RS is the most stable structure of ScN as it was reported in the other works [1, 3–11]. The cohesive energies of ScN are calculated to be –12.40, –13.87, –14.06 and –14.48 eV for B2, B3, B4 type metastable and B1 type most stable structures, respectively. In the cohesive energy calculations [equation (2.1)], the atomic self-energies of Sc and N atoms are calculated to be –1528.609 and –109.136 Ry, respectively. The present cohesive energies are found to be different (∼1 eV) from the ones [9, 10] defined by only the minimum total energies (per unit cell) of the structures.

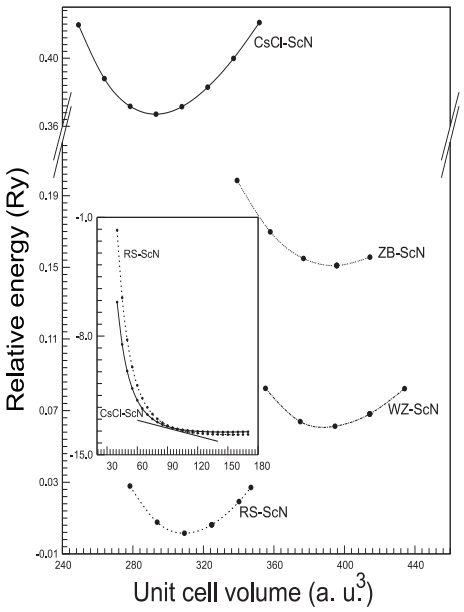

Figure 2. The relative total energy (per unit cell) versus volume within EV_{ex}-PW_{co}-GGA for ScN in RS, WZ, ZB, and CsCl structures. The inset figure displays the cross point on the variation of the total energies (per unit cell) of the RS-ScN (dotted line) and CsCl-ScN (solid line) structures as a function of volume.

The equilibrium lattice constants, bulk moduli, and first order pressure derivative of the bulk moduli of ScN in B1-B4 phases calculated within LDA, PBE-GGA, EV_{ex}-PW_{co}-GGA, and EV_{ex}-GGA-LDA_{co} schemes are tabulated in table 1, together with the available measured and calculated values of the other groups, for comparison. The equilibrium lattice constants of 4.510 and 4.513 Å obtained for RS-ScN structure by EV_{ex}-PW_{co}-GGA and PBE-GGA calculations, respectively, are found to be very close to the measured values of 4.501 [1] and 4.5 Å [3–8]. On the other hand, the equilibrium lattice constant of RS-ScN obtained by the present EV_{ex}-PW_{co}-GGA and PBE-GGA calculations are found to be very close to the values calculated by FP-LAPW and ab-initio PP methods within PBE-GGA and PCVJPSF (Perdew-Chevary-Vosko-Jackson-Pederson-Singh-Fiolhais)-GGA [39] schemes [10, 12, 13]. The present bulk moduli of 202.35 and 195.95 GPa found for RS-ScN within EV_{ex}-PW_{co}-GGA and PBE-GGA's, respectively, are the best ones providing the measured value of 182∓40 GPa [1]. The present bulk moduli of EV_{ex}-PW_{co}-GGA and PBE-GGA's are also found to be in the range of 196–202 GPa defined by the corresponding results of ab-initio PP and FP-LAPW calculations within PBE-GGA and PCVJPSF-GGA

Table 1. The optimized lattice constant [a(Å)], bulk modulus [B(GPa)], and first-order pressure derivative of bulk modulus [$B^{'}$] calculated by LDA (I), PBE-GGA (II), EV_{ex}-PW_{co}-GGA (III), and EV_{ex}-GGA-LDA_{co} (IV) approaches for ScN in RS, CsCl, ZB, and WZ phases.

		Present Work				Other Works	
		I	II	III	IV	Theor.	Exp.
RS-ScN	a	4.432	4.513	4.510	4.755	$4.44^{9}, 4.54^{9}$ $4.520^{10}, 4.651^{11}$ $4.42^{12}, 4.51^{13}$ $4.50^{12,14,15}$ $4.455^{14}, 4.533^{14}$	4.501^{1} 4.5^{3-8}
	B	230.44	195.95	202.35	137.35	$220^{9}, 201^{9,12}$ 201.576^{10} $210.364^{11}, 235^{12}$ $197^{13}, 221^{14}$ 196^{14}	182 ∓ 40^{1}
	$B^{'}$	4.41	4.31	4.25	4.16	$3.31^{9}, 3.89^{10,13}$ $3.12^{11}, 4.27^{14}$ 4.36^{14}	
CsCl-ScN	a	2.727	2.787	2.788	2.961	$2.81^{9}, 2.79^{10}, 2.926^{11}$	
	B	212	182	180	118	$170^{9}, 178.60^{10}, 159.759^{11}$	
	$B^{'}$	4.04	4.28	4.15	3.93	$3.47^{9}, 4.43^{10}, 3.034^{11}$	
ZB-ScN	a	4.804	4.893	4.888	5.142	$4.88^{9}, 4.939^{11}$	
	B	159.12	141.18	142.35	89.83	$153^{9}, 145.195^{11}$	
	$B^{'}$	3.85	3.79	3.77	5.06	$3.34^{9}, 3.43^{11}$	
WZ-ScN	a	3.424	3.497	3.494	3.680	$3.49^{9}, 3.45^{11}$	
	c/a	1.578	1.582	1.581	1.581	$1.6^{9}, 1.552^{11}$	
	u	0.389	0.389	0.389	0.387	$0.38^{9}, 0.377^{11}$	
	B	146	131	131	86	$156^{9}, 132.91^{11}$	
	$B^{'}$	4.18	3.93	3.43	3.88	$2.16^{9}, 3.29^{11}$	

schemes [9, 10, 12–14]. The equilibrium lattice constants and bulk moduli of RS-ScN calculated by LDA and EV_{ex}-GGA-LDA_{co}'s are either underestimated or overestimated with respect to the measured ones given in table 1. The values of the first order pressure derivative of the bulk moduli (table 1) presented for RS-ScN are all close to each other and in agreement with the results of ab-initio PP calculations of LDA and PBE-GGA's [14]. As it is determined for ScN in RS phase, the structural features of ScN in B2-B4 phases calculated by EV_{ex}-PW_{co}-GGA and PBE-GGA's are very close to each other (table 1). The present equilibrium lattice constants, bulk moduli, and first order pressure derivatives of the bulk moduli of ScN in B2-B4 phases could not be compared, because of the lack of the measured ones in the literature. But, they are (especially the results of LDA, PBE-GGA and EV_{ex}-PW_{co}-GGA) comparable with the results of the other groups calculated within LDA [9, 11] and PBE-GGA [9, 10] schemes.

The total energies (per unit cell) of RS-ScN and CsCl-ScN relative to a reference total energy are plotted in the small frame of figure 2 for low unit cell volumes of the structures. The crossing of the total energy curves observed in the inset figure indicates the phase transition from RS to CsCl structure at high pressure. The enthalpy of the RS phase equals to that of the CsCl phase

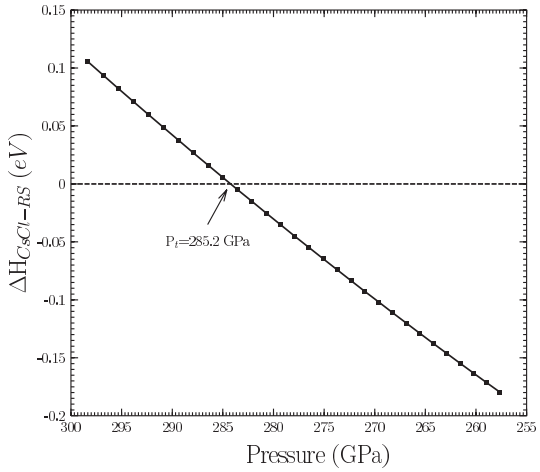

Figure 3. The difference of enthalpy between the CsCl and RS phases ($\Delta H_{CsCl-RS}$) versus pressure.

at the cross point. Therefore, the necessary pressure providing the transition from RS to CsCl corresponds to the zero difference between the enthalpy of the structures. The enthalpy of the RS and CsCl phases is evaluated by Gibb's free energy

$$H = E_{\text{tot}} + PV - TS \tag{3.1}$$

at T=0 K. In figure 3, the difference between the enthalpy of the CsCl and RS structures ($\Delta H_{\text{CsCl-RS}}$) decreases to zero at the transition pressure of 285.2 GPa. The present transition pressure is found to be smaller than the ones (341 GPa [9], 332.75 GPa [11]) calculated directly from the slope of the common tangent.

3.2. Electronic properties

The electronic band structures of ScN in RS, CsCl, ZB, and WZ phases have been calculated along the various symmetry lines within LDA, PBE-GGA, EV_{ex}-PW_{co}-GGA, and EV_{ex}-GGA-LDA_{co} schemes. The energy gaps of the RS-ScN correspond to different symmetry directions, and the points are tabulated in table 2, together with the available measured and calculated energy gaps of the other groups, for comparison. The electronic band structure calculations of RS-ScN phase have given the top of the valence band at Γ point. The bonding analysis given in [40] has shown that RS-AlN has three *p*-like bonding, three *d*-like antibonding t_{2g}, and two *d*-like nonbonding e_g bands formed by the hybridization of three-valence *p* states of N with the five *d* states of Sc. According to the present partial density of states (DOS) calculations plotted in figure 4, the upper valence bands are formed mainly by the N *p*-orbitals with some mixture of Sc *d*-orbitals, while the conduction bands are predominantly originated from Sc *d*-t_{2g} states with some admixture of the Sc *d*-e_g and N *p*-states. The minimum of the conduction band is mainly of Sc 3*d* character. The present identification for the conduction and valance bands of ScN is consistent with the partial density of states analysis given in [14]. The present LDA and PBE-GGA calculations have given the negative indirect gap at X point for RS-ScN. The negative or approximately zero indirect gap at X point was also reported in [9–14] for RS-ScN by the same approximations. The indirect energy gap of RS-ScN is 0.46 and 0.62 eV by the present calculations of EV_{ex}-PW_{co}-GGA and EV_{ex}-GGA-LDA_{co}'s, respectively. Therefore, EV_{ex}-PW_{co}-GGA and EV_{ex}-GGA-LDA_{co}'s are found to be more accurate than PBE-GGA to produce a positive indirect gap for ScN in RS phase. These indirect gap values obtained by the present non-corrected EV_{ex}-PW_{co}-GGA and EV_{ex}-GGA-LDA_{co} calculations are in agreement with the value of 0.54 eV reported by non-corrected PP-GGA calculations [15]. In the literature, different correction approximations used in LDA and GGA schemes were found

Table 2. The calculated and experimental energy band gaps [E_g(eV)] of RS-ScN.

Approach	$E_g^{\Gamma-\Gamma}$	E_g^{X-X}	E_g^{W-W}	$E_g^{\Gamma-X}$	$E_g^{\Gamma-K}$	E_g^{X-W}
LDA[a]	2.40	0.68	6.43	− 0.24	3.69	4.61
PBE-GGA[a]	2.43	0.91	6.22	− 0.01	3.59	4.52
EV_{ex}-PW_{co}-GGA[a]	2.60	1.33	6.17	0.46	3.73	4.60
EV_{ex}-PW_{co}-GGA+U[a]	3.28	1.82	6.81	0.90	4.33	5.25
EV_{ex}-GGA-LDA_{co}[a]	2.29	1.46	5.37	0.62	3.19	4.03
GGA[9]	2.40	0.90	6.40	0.0	2.30	
GGA[10]		0.9		~ 0.0		
LDA[11]				~ 0.0		
LDA[12]				0.0		
sX-LDA[12]		2.41		1.58		
GGA[13]	2.41	0.90	6.21	0.02	2.22	
LDA[14]	2.34	0.75		− 0.15		
GGA[14]	2.43	0.87		− 0.03		
OEPx(cLDA)−G_oW_o[14]	3.51	1.98		0.84		
LDA−G_oW_o[14]	3.71	2.06		1.14		
OEPx(cLDA)[14]	4.53	2.59		1.70		
GGA[15]				0.54		
EXX-GGA[20]	4.70	2.90		1.60		
LDA−GW[21]	4.3	2.0		0.9		
exp.[3]		1.8 − 2.1				
exp.[4]		2.1				
exp.[7]	2.1 − 2.4	2.15		0.9 ∓ 0.1		
exp.[8]	> 2.6			2.4		
exp.[20]	~ 3.8	2.4 ∓ 0.3		1.3 ∓ 0.3		

[a] present work

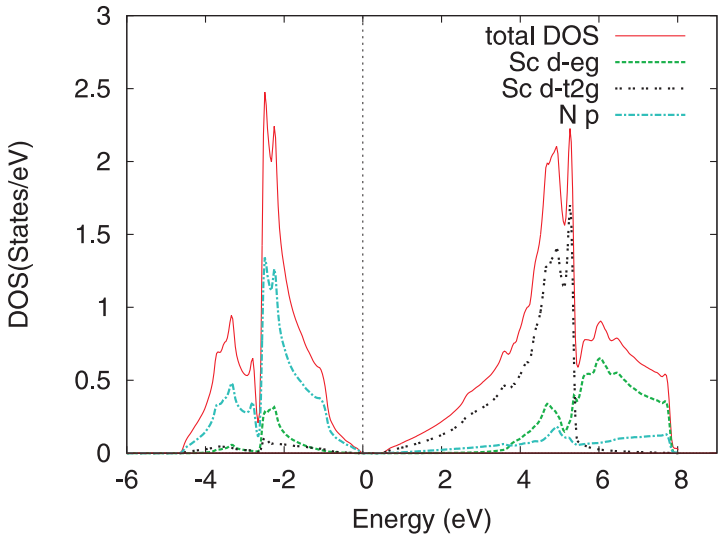

Figure 4. (Color on-line) The total and partial DOS within EV_{ex}-PW_{co}-GGA for RS-ScN.

to be effective to produce a larger indirect gap close to the measured value of ∼1 eV for RS-ScN [12, 14, 20, 21]. The present EV_{ex}-PW_{co}-GGA+U^{SIC} calculations have also improved the highest valence and lowest conduction band states of RS-ScN by giving an indirect gap of 0.9 eV. It is found that the corrected Coulomb interaction term by the U parameter of 4.08 eV pushes the N $2p$ bands down and Sc $3d$-t_{2g} bands up in the present EV_{ex}-PW_{co}-GGA+U^{SIC} calculations to enlarge the indirect energy gap by an amount of 0.44 eV. Since the valence and conduction bands in RS-ScN structure are formed by the hybridization of d-orbitals of Sc and p-orbitals of N atoms [40], the correction on the Coulomb self- and exchange-correlation interactions of the localized d-orbitals of Sc in EV_{ex}-PW_{co}-GGA+U^{SIC} calculations has indirectly improved N $2p$ bands. In the same correction method, the direct band gap of RS phase at X point is calculated to be 1.82 eV with respect to the measured and calculated values in the ranges of 1.8–2.4 eV [3, 4, 7, 20] and 1.98–2.90 eV [12, 14, 20, 21], respectively. The present Γ point direct energy gap of 3.28 eV for B1 phase is found to be comparable with the results of optical transmission [8] and reflection [20] measurements and OEPx(cLDA)-G_oW_o [14] and LDA-G_oW_o [14] calculations (table 2). The present electronic band structure of RS-ScN within EV_{ex}-PW_{co}-GGA scheme is plotted in figure 5. The improvement of the band structure due to EV_{ex}-PW_{co}-GGA+U^{SIC} calculations is also shown in the same plot.

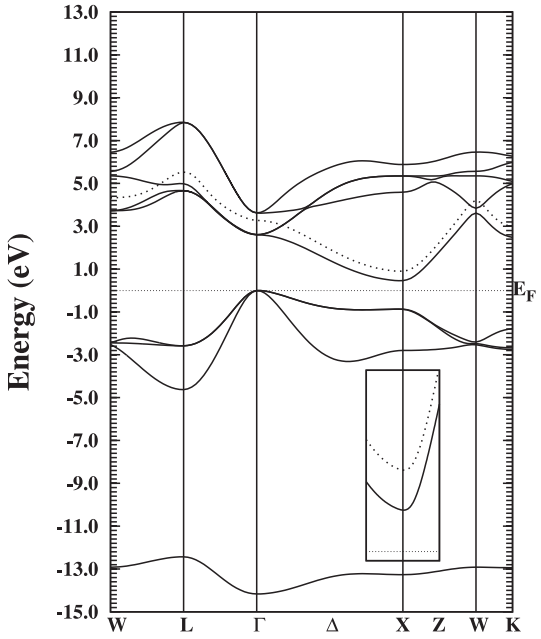

Figure 5. Electronic band structure of RS-ScN within EV_{ex}-PW_{co}-GGA. The dotted line shows the correction of the conduction band state within EV_{ex}-PW_{co}-GGA+U^{SIC} calculations.

In this work, the effective electron and hole masses (heavy and light) are calculated using the electronic band structure of RS-ScN obtained by EV_{ex}-PW_{co}-GGA+U^{SIC} scheme (figure 5). The conduction band and valance band effective masses at the X and Γ points, respectively, are calculated by fitting a quadratic function to the corresponding band structure energies. The closely spaced k points in a very small range around the X point have yielded the electron effective mass of $0.22\,m_e$. The electron effective mass in RS-ScN was determined between 0.1 and $0.2\,m_e$ by extrapolating the measured values of infrared reflectivity for high carrier concentrations to low ones [41]. Since the edge of the conduction band along Δ(Γ-X) and Z (W-X) directions approaches the X point with quiet different slopes (inset plot in figure 5), the electron effective mass is also calculated along Δ and Z directions, separately. The electron effective masses are calculated to be $1.621\,m_e$ and $0.223\,m_e$ along Δ and Z directions around X point with respect to the ones reported in the range of 1.441–$1.625\,m_e$ and 0.124–$0.253\,m_e$, respectively, by LDA [7, 14], GGA [14], OEPx(cLDA) [14], and OEPx(cLDA)-G_oW_o [14] schemes. In the present work, the effective mass for the heavy and light holes are calculated to be 0.93 and $0.19\,m_e$ at Γ point, respectively.

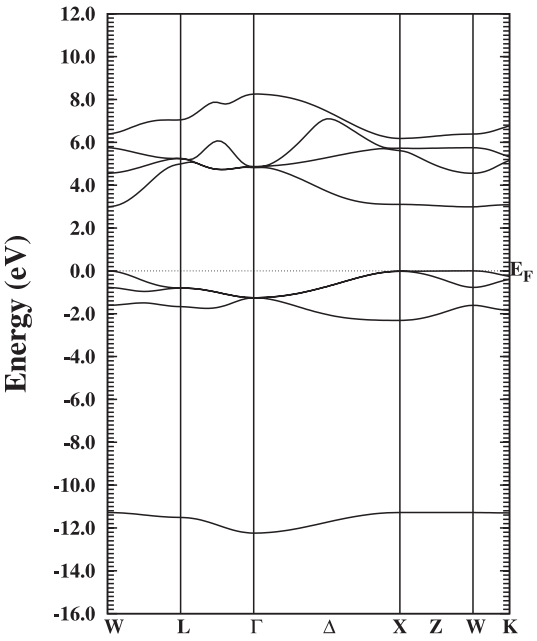

Figure 6. Electronic band structure of ZB-ScN within EV_{ex}-PW_{co}-GGA.

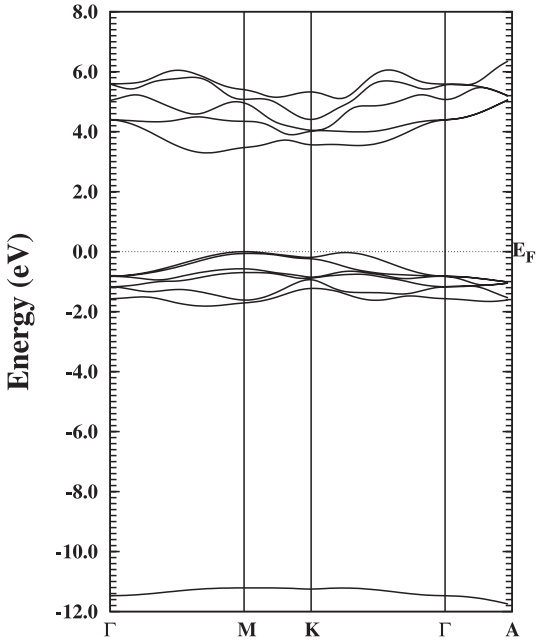

Figure 7. Electronic band structure of WZ-ScN within EV_{ex}-PW_{co}-GGA.

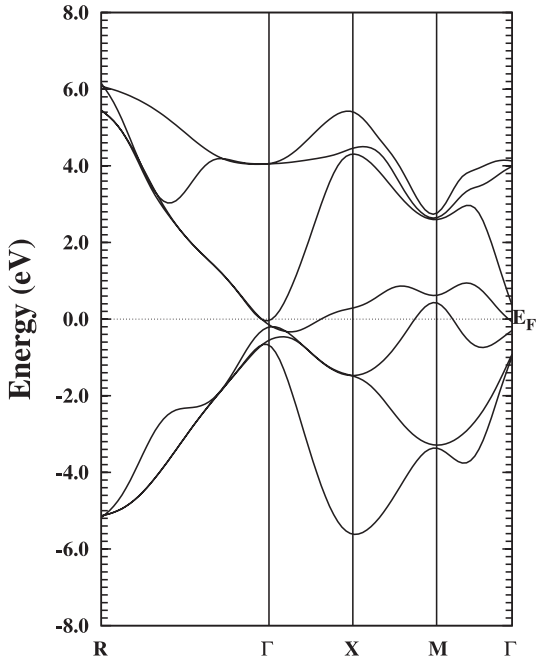

Figure 8. Electronic band structure of CsCl-ScN within EV_{ex}-PW_{co}-GGA.

The electronic band structures of ScN in B2-B4 metastable phases have been also calculated by LDA, PBE-GGA, EV_{ex}-PW_{co}-GGA, and EV_{ex}-GGA-LDA_{co} schemes. The band structures of the ZB, WZ, and CsCl phases calculated by EV_{ex}-PW_{co}-GGA are plotted in figures 6–8. The energy gaps of the ZB and WZ metastable structures correspond to different symmetry lines, and the points are tabulated in table 3. The calculations have yielded non-metallic band structures for

Table 3. The energy band gaps [E_g(eV)] of ZB-ScN and WZ-ScN phases calculated by LDA (I), PBE-GGA (II), EV_{ex}-PW_{co}-GGA (III), and EV_{ex}-GGA-LDA_{co} (IV) approaches.

Phase	Approach	$E_g^{\Gamma-\Gamma}$	E_g^{X-X}	E_g^{W-W}	E_g^{L-L}	$E_g^{\Gamma-X}$	$E_g^{\Gamma-W}$	$E_g^{\Gamma-L}$	$E_g^{W-\Gamma}$	E_g^{W-L}	E_g^{W-X}
ZB	I	5.27	2.39	2.30	5.80	3.80	3.72	6.28	3.86	4.87	2.38
	II	4.94	2.50	2.44	5.56	3.73	3.67	6.00	3.71	4.77	2.50
	III	6.05	3.12	3.00	5.78	4.36	4.24	6.24	4.80	4.98	3.10
	IV	5.07	2.90	2.82	4.93	3.83	3.75	5.29	4.14	4.36	2.90
		$E_g^{\Gamma-\Gamma}$	E_g^{M-M}	E_g^{K-K}	$E_g^{\Gamma-M}$	$E_g^{\Gamma-K}$	E_g^{A-A}	$E_g^{M-\Sigma}$	E_g^{M-K}	$E_g^{M-\Gamma}$	E_g^{M-A}
WZ	I	5.11	2.96	3.53	3.92	4.17	6.42	2.79	3.21	4.15	5.20
	II	4.75	3.05	3.51	3.85	3.24	6.08	2.88	3.24	3.94	5.05
	III	5.22	3.47	3.76	4.29	4.36	6.16	3.29	3.54	4.39	5.12
	IV	4.51	3.23	3.44	3.81	3.85	5.24	3.08	3.26	3.93	4.49

ZB-ScN and WZ-ScN with the top of the valence band at W and M symmetry points, respectively. The ZB-ScN structure is found to be a direct band gap material even if the direct (E_g^{W-W}) and indirect (E_g^{W-X}) band gaps are very close to each other. However, ZB-ScN was an indirect band gap (E_g^{X-W}) material in [9, 11]. In reference [9], the ZB-ScN structure was a direct band gap (E_g^{W-W}) material when the electronic band structures were calculated with the lattice constant of RS-ScN. The present direct band gap energies of PBE-GGA (2.44 eV) and LDA (2.30 eV) schemes for ZB structure are found to be comparable with the corresponding values of 2.4 and 2.36 eV given by similar approximations [9, 11]. The present direct band gap of ZB phase at W point is enlarged to ∼3 eV by EV_{ex}-PW_{co}-GGA (3 eV) and EV_{ex}-GGA-LDA_{co} (2.82 eV) calculations. The indirect band gap of WZ phase is calculated to be ∼3 eV along M-Σ direction by LDA and PBE-GGA schemes. The large indirect band gap of ScN in WZ structure was also reported in [9]. As it is found for ZB structure, the indirect band gap of WZ-ScN is enlarged by EV_{ex}-PW_{co}-GGA (3.29 eV) and EV_{ex}-GGA-LDA_{co} (3.08 eV)'s. According to all approximations considered in this work, ScN in CsCl phase has a metallic band structure (figure 8) as it was reported earlier by LDA and GGA calculations [9, 11]; the conduction and valance bands are observed to be mixed completely. Because of the lack of the measurements on metastable structures of ScN, the present results are compared only by the calculated ones.

4. Summary and conclusion

A comparative study by FP-LAPW calculations based on DFT within LDA, PBE-GGA, EV_{ex}-PW_{co}-GGA, and EV_{ex}-GGA-LDA_{co} schemes is introduced for the structural and electronic properties of ScN in RS, CsCl, ZB, and WZ phases. According to all approximations used in this work, the RS phase is a stable ground state structure and makes a transition to CsCl phase at high transition pressure. It can be concluded that EV_{ex}-PW_{co}-GGA is the best one among the others to provide accurate structural features and non-zero, positive indirect band gap of RS-ScN comparable with the experimental results when the structural and electronic calculations are aimed to be calculated by the same exchange-correlation energy approximation. Although LDA and PBE-GGA's have calculated good structural features, they have yielded a small negative indirect band

gap for RS-ScN. On the other hand, EV_{ex}-GGA-LDA_{co} has roughly supplied the lattice constant and bulk modulus but it is found to be very accurate for the electronic features of RS-ScN. The indirect band gap of ScN in RS phase is enlarged to the corresponding measured value by EV_{ex}-PW_{co}-GGA+U^{SIC} calculations in which the Coulomb self- and exchange-correlation interactions of the localized *d*-orbitals of Sc have been corrected by the potential parameter of U. The present EV_{ex}-PW_{co}-GGA calculations have also provided good results for the structural and electronic features of ZB, WZ and CsCl phases comparable with the theoretical data reported in the literature. Therefore, EV_{ex}-PW_{co}-GGA and EV_{ex}-PW_{co}-GGA+U^{SIC} can be considered to be good exchange-correlation energy approximations for further works of ScN.

References

1. Gall D., Petrov I., Hellgren N., Hultman L., Sundgren J.E., Greene J.E., J. Appl. Phys., 1998, **84**, 6034; doi:10.1063/1.368913.
2. Edgar J.H., Bohnen T., Hageman P.R., J. Cryst. Growth, 2008, **310**, 1075; doi:10.1016/j.jcrysgro.2007.12.053.
3. Dismukes J.P., Yim W.M., Ban V.S., J. Cryst. Growth, 1972, **13/14**, 365; doi:10.1016/0022-0248(72)90185-6.
4. Moustakas T.D., Dismukes J.P., Pearton S.J., Electrochem. Soc. Proc., 1996, **96-11**, 197.
5. Al-Brithen H.A., Smith A.R., Appl. Phys. Lett., 2000, **77**, 2485; doi:10.1063/1.1318227.
6. Smith A.R., Al-Brithen H.A., Ingram D.C., Gall G., J. Appl. Phys., 2001, **90**, 1809; doi:10.1063/1.1388161.
7. Al-Brithen H.A., Smith A.R., Gall D., Phys. Rev. B, 2004, **70**, 045303; doi:10.1103/PhysRevB.70.045303.
8. Gregoire J.M., Kirby S.D., Turk M.E., van Dover R.B., Thin Solid Films, 2009, **517**, 1607; doi:10.1016/j.tsf.2008.09.076.
9. Takeuchi N., Phys. Rev. B, 2002, **65**, 045204; doi:10.1103/PhysRevB.65.045204.
10. Maachou A., Amrani B., Driz M., Physica B, 2007, **388**, 384; doi:10.1016/j.physb.2006.06.145.
11. Tebboune A., Rached D., Benzair A., Sekkal N., Belbachir A.H., Phys. Stat. Sol. (b), 2006, **243**, 2788; doi:10.1002/pssb.200541356.
12. Stampfl C., Mannstadt W., Asahi R., Freeman A.J., Phys. Rev. B, 2001, **63**, 155106; doi:10.1103/PhysRevB.63.155106.
13. Duman S., Bağci S., Tütüncü H.M., Uğur G., Srivastava G.P., Diam. Relat. Mater., 2006, **15**, 1175; doi:10.1016/j.diamond.2005.12.003.
14. Qteish A., Rinke P., Scheffler M., Neugebauer J., Phys. Rev. B, 2006, **74** 245208; doi:10.1103/PhysRevB.74.245208.
15. Houari A., Matar S.F., Belkhir M.A., Comp. Mater. Sci., 2008, **43** 392; doi:10.1016/j.commatsci.2007.12.005.
16. Perdew J. P., Wang Y., Phys. Rev. B, 1992, **45**, 13244; doi:10.1103/PhysRevB.45.13244.
17. Hedin L., Lundqvist B.I., J. Phys. C, 1971, **4**, 2064; doi:10.1088/0022-3719/4/14/022.
18. Perdew J.P., Jackson K.A., Pederson M.R., Singh D.J., Fiolhais C., Phys. Rev. B, 1992, **46**, 6671; doi:10.1103/PhysRevB.46.6671.
19. Perdew J.P., Burke S., Ernzerhof M., Phys. Rev. Lett., 1996, **77**, 3865; doi:10.1103/PhysRevLett.77.3865.
20. Gall D., Städele M., Järrendahl K., Petrov I., Desjardins P., Haasch R.T., Lee T.-Y., Greene J.E., Phys. Rev. B, 2001, **63**, 125119; doi:10.1103/PhysRevB.63.125119.
21. Lambrecht Walter R.L., Phys. Rev. B, 2000, **62**, 13538; doi:10.1103/PhysRevB.62.13538.
22. Hedin L., Phys. Rev. B, 1965, **139**, A796; doi:10.1103/PhysRev.139.A796.
23. Städele M., Majewski J.A., Vogl P., Görling A., Phys. Rev. B, 1999, **59**, 10031; doi:10.1103/PhysRevB.59.10031.
24. Bechstedt F., Del Sole R., Phys. Rev. B, 1998, **38**, 7710; doi:10.1103/PhysRevB.38.7710.
25. Asahi R., Mannstadt W., Freeman A.J., Phys. Rev. B, 1999, **59**, 7486; doi:10.1103/PhysRevB.59.7486.
26. Paduani C., Solid State Commun., 2008, **148**, 297; doi:10.1016/j.ssc.2008.09.010.
27. Zaoui A., Kacimi S., Bouhortt A., Bouhafs B., Physica B, 2010, **405**, 153; doi:10.1016/j.physb.2009.08.040.

28. Kityk I.V., Comp. Mater. Sci., 2003, **27**, 342; doi:10.1016/S0927-0256(03)00039-9; Mater. Lett., 2003 **57**, 1798; doi:10.1016/S0167-577X(02)01071-6.
29. Anisimov Vladimir I., Zaanen Jan, Andersen Ole K., Phys. Rev. B, 1991, **44**, 943; doi:10.1103/PhysRevB.44.943.
30. Blaha P., Schwarz K., Madsen G.K.H., Kvasnicka D., Luitz J., WIEN2k, An Augmented-Plane-Wave + Local Orbitals Program for Calculating Crystal Properties, Karlheinz Schwarz, Techn. Universität, Wien, Austria, 2001, ISBN 3–9501031–1–2.
31. Engel E., Vosko S.H., Phys. Rev. B, 1993, **47**, 13164; doi:10.1103/PhysRevB.47.13164.
32. Perdew J.P., Wang Y., Phys. Rev. B, 1986,**33**, 8800; doi:10.1103/PhysRevB.33.8800; Perdew J.P. Electronic Structure of Solids, ed. P. Ziesche and H. Eschring, Academic, Berlin, 1991.
33. Pemmaraju C.D., Archer T., Sánchez-Portal D., Sanvito S., Phys. Rev. B, 2007, **75**, 045101; doi:10.1103/PhysRevB.75.045101.
34. Wu S.Q., Zhu Z.Z., Yang Y., Hou Z.F., Comp. Mater. Sci., 2009, **44**, 1243; doi:10.1016/j.commatsci.2008.08.014 .
35. Cai T., Han H., Yu Y., Gao T., Du J., Hao L., Physica B, 2009, **404**, 89; doi:10.1016/j.physb.2008.10.009.
36. Blaha P., Schwarz K., Novák P., Int. J. Quantum Chem., 2005, **101**, 550; doi:10.1002/qua.20310.
37. Anisimov Vladimir I., Aryasetiawanz F., Lichtenstein A.I., J. Phys.: Condens. Matter, 1997, **9**, 767; doi:10.1088/0953-8984/9/4/002.
38. Murnaghan F.D., Proc. Natl. Acad. Sci. USA, 1944, **30**, 244; doi:10.1073/pnas.30.9.244.
39. Perdew J.P., Jackson K.A., Pederson M.R., Singh D.J., Fiolhais C., Phys. Rev. B, 1992, **46**, 6671; doi:10.1103/PhysRevB.46.6671.
40. Harrison A., Straub G.K., Phys. Rev. B 1987, **36**, 2695; doi:10.1103/PhysRevB.36.2695.
41. Harbeke G., Meier E., Dismukes J.P., Opt. Commun., 1972, **4**, 335; doi:10.1016/0030-4018(72)90071-5.

Порівняльне дослідження структурних і електронних властивостей монокристалічного ScN

Р. Могаммад[1,2], С. Катірчіоглу[2]

[1] Палестинський технічний університет, коледж прикладних наук, ВестБенк, Палестина

[2] Близькосхідний технічний університет, фізичний факультет, 06530 Анкара, Туреччина

Представлено порівняльне дослідження за допомогою FP-LAPW розрахунків, що базуються на теорії функціоналу густини (DFT) в рамках схем LDA, PBE-GGA, EV_{ex}-PW_{co}-GGA, і EV_{ex}-GGA-LDA_{co} для структурних і електронних властивостей ScN в фазах RS, ZB, WZ і CsCl. Відповідно до всіх наближень, виконаних в цій роботі, фаза RS є стійкою структурою в основному стані і здійснює перехід у фазу CsCl при високому тиску. В той час як схеми PBE-GGA і EV_{ex}-PW_{co}-GGA забезпечують кращі структурні властивості такі як рівноважна постійна ґратки і об'ємні модулі, лише схеми EV_{ex}-PW_{co}-GGA та EV_{ex}-GGA-LDA_{co}'s дають ненульову, позитивну непряму енергетичну щілину для RS-ScN, порівняльну з експериментальними. Непряма зонна щілина ScN в фазі RS є збільшена до відповідного виміряного значення за допомогою EV_{ex}-PW_{co}-GGA+U^{SIC} обчислень, в яких кулонівські власні і обмінні кореляційні взаємодії локалізованих d-орбіталей Sc були поправлені за допомогою параметра потенціалу U. Розрахунки EV_{ex}-PW_{co}-GGA також приводять до добрих результатів для структурних і електронних характеристик ScN у фазах ZB, WZ і CsCl, якщо порівнювати з теоретичними даними, наявними в літературі. Вважається, що схеми EV_{ex}-PW_{co}-GGA та EV_{ex}-PW_{co}-GGA+U^{SIC} є найкращими серед інших у випадку, коли обчислюються структурні та електронні характеристики ScN в рамках тих же наближень для енергії обмінної кореляції.

Ключові слова: *ScN, FP-LAPW, DFT, структурні властивості, електронні властивості*